AIMS Mathematics, 9(9): 24832–24853.
DOI: 10.3934/math.20241209
Received: 28 June 2024
Revised: 19 August 2024
Accepted: 20 August 2024
Published: 23 August 2024

https://www.aimspress.com/journal/Math

Research article

Resonance analysis and time-delay feedback controllability for a fractional horizontal nonlinear roller system

Zhoujin Cui[1], **Xiaorong Zhang**[2] **and Tao Lu**[1,*]

[1] School of Mathematical Sciences, Jiangsu Second Normal University, Nanjing, 210013, China
[2] School of Economics and Management, Jiangsu Maritime Institute, Nanjing, 211170, China

* **Correspondence:** Email: lutao@jssnu.edu.cn.

Abstract: In this paper, we investigated the nonlinear vibration characteristics and time-delay feedback controllability of a fractional horizontal roll system, which is described by a fractional Duffing-van der Pol oscillator under an external harmonic excitation. We focused on the resonance of fractional roller systems and conducted corresponding vibration control. The amplitude-frequency equations of primary resonance and superharmonic resonance were obtained using the multiple scale method. The amplitude-frequency characteristic curves of the system with different parameters were presented, and the influence of system parameters on the curves was analyzed. In addition, the time-delay feedback controller was designed to control the parameter excitation vibration. The numerical simulation results have verified the effectiveness of the time-delay controller in eliminating the jumping and hysteresis phenomena of the rolling system. The comparisons of approximate analytical solution and numerical solution was fulfilled, and the result certifies the correctness and satisfactory precision of the approximately analytical solution. The analysis results provide certain theoretical guidance for the vibration reduction of the horizontal nonlinear roller system.

Keywords: fractional horizontal nonlinear roller system; primary resonance; superharmonic resonance; multiple scale method
Mathematics Subject Classification: 34A08, 37N35

1. Introduction

Rolling mill is a key equipment in the steel industry and an important equipment in the modern heavy machinery field. It is a complex working system, and its safe and stable operation is crucial to ensure efficient production of rolled products. With the development of society, higher requirements have been put forward for the surface quality of strip mills, so the requirements of high precision and high dynamic performance have been promoted for rolling mills [1]. However, the high rolling

speed and strength of modern rolling mills often result in unstable rolls during the rolling process. For example, due to the presence of many nonlinear factors within the system, the rolling mill roll system exhibits complex nonlinear vibration characteristics. When rolling high strength and thin strip steel, the mill frequently appears "ghost" vibration, which mostly includes vertical vibration, horizontal vibration, axial oscillation, transverse and longitudinal vibration of the strip steel, torsional vibration, and axial vibration of the main drive system [2]. These vibrations seriously affect the working performance and reliability of the rolling mill system and restrict the stability of the rolling production process [3,4]. Therefore, it is necessary to strengthen the analysis and study of the vibration causes of rolling mill and deal with the problems in time to ensure the stable operation of the equipment.

The study of nonlinear dynamics of vibration in rolling systems has attracted widespread attention and has been ongoing for decades. Many experts and scholars have conducted many beneficial exploratory studies from various angles. These researchers mainly focus on why rolling mills vibrate, how they vibrate, and how to suppress vibration (see [5–13] and the reference therein). The authors in [5] assumed that the workpiece is an elastic part with linear stiffness and established a linear vertical vibration model for the rolling mill frame based on linear vibration theory. In order to study the vibration characteristics of the rolling mill, the authors in [6] studied the effect of tension on nonlinear vibration of rolling mills. By changing the external excitation frequency to analyze the stability of the rolling mill vibration system, it was concluded that rolling speed and strip thickness have a significant impact on system stability. A horizontal friction vibration model of the rolling mill rolls was established in [7], and simulation analysis was conducted under the conditions of eliminating the bearing clearance of the rolling mill frame and adding a floating support for the coupling. By analyzing the effects of changes in workpiece thickness and motor speed on the connection angle and roll gap friction, a nonlinear torsional vibration model of the rolling mill was established in [9], indicating that reducing damping coefficient and nonlinear stiffness helps to reduce vibration intensity. In terms of research on vibration control, the authors in [11] designed a global sliding mode controller for the rolling mill drive system to suppress the uncertainty of rolling parameters and achieved good tracking performance. In [12], a displacement time-delay feedback link was introduced to control the vibration of the roller system, and different time-delay parameters were selected to test the control effect. The research results indicated that appropriate time-delay feedback parameters can suppress the unstable vibration of the roller system. The authors in [13] studied the vibration characteristics of the corrugated roller system and designed a time-delay feedback controller to control the parameter excitation vibration of the system.

In recent years, fractional calculus and its application in different fields have attracted widespread attention, providing a very useful mathematical tool for describing the memory and genetics of various materials and processes, such as fractional modeling of robotic manipulator [14], bibliographic analysis on artificial neural networks based on fractional calculus [15], fractional model of cerebral aneurysm [16], fractional model of ENSO phenomenon [17], fractional mechanics [18], fractional memristor circuit [19], fractional infectious disease model [20], and so on. Even if all individuals in the system have integer order dynamic characteristics, the overall dynamic characteristics of the system may still be fractional order. It can better describe the viscoelasticity of materials, such as suspension [21], air spring [22], magneto rheological damper [23] and hydraulic bushing [24]. In the research of rolling systems, fractional calculus has also begun to be involved [25–28]. Among them, the authors in [26, 27] introduced a fractional derivative term when establishing a horizontal nonlinear

vibration model for rolling mills. In [28], the resonance characteristics of the fractional roller system under high-frequency and low-frequency excitation signals were studied.

With the continuous development of active control technology, there is an increasing amount of research on actively utilizing time-delay feedback to achieve various control objectives. Time-delayed feedback control, as an effective control method, has been widely applied in the field of vibration control [29–31]. Adding fractional order factors to the simulation of rolling mill systems is more reasonable, but there are many problems that need to be solved urgently in the current research on fractional order nonlinear systems. For example, complex dynamic characteristics such as the influence of system parameters on periodic solutions under time-delay feedback, as well as many problems such as bifurcation control, require further research. Therefore, based on the superiority of fractional calculus and time-delayed feedback control, it is necessary to study the dynamic characteristics of fractional order nonlinear rolling systems and the bifurcation control problem under time-delayed feedback, which has important theoretical significance and application value. Motivated by [13,26–28], we focus on the vibration characteristics of the system and time-delay feedback controllability of the horizontal nonlinear roller system, and corrects the expression errors in existing literature. The innovation lies in systematically studying the resonance of fractional roller systems and conducting corresponding vibration control, further validating the effectiveness of the theoretical research through numerical simulation, providing new ideas for the research of roller system vibration theory.

The paper is organized as follows: In the second section, the fractional derivative term is considered in the horizontal nonlinear roller system, and the nonlinear vibration model is established. In the third section, the amplitude-frequency response equations of the primary resonance and time-delay feedback control are obtained using the multiple scale method, and numerical analysis is conducted. In the fourth section, we mainly present the amplitude-frequency response equations of the secondary resonance and time-delay feedback control and analyze the numerical simulation results to verify the effectiveness of theoretical research. The comparison of approximate analytical solution and numerical solution is fulfilled in the fifth section. In the last section, we conclude this paper.

2. Nonlinear vibration model

2.1. Problem formulation

Referring to the model of the horizontal roller system in [26–28], in order to study the nonlinear vibration characteristics of the strip rolling mill in the horizontal direction, the Duffing and the Van der Pol oscillators were introduced, and the nonlinear damping and stiffness within interface of the rolling mill were considered to establish a fractional horizontal nonlinear parametric vibration model for the rolling mill work roll, as shown in Figure 1.

The vibration model can be given by a second-order non-autonomous differential equation as follows

$$m\ddot{x} + c(x^2 - 1)\dot{x} + KD_t^q x + (k_1 + k_2x^2)x = F\cos\omega t, \tag{2.1}$$

where x is the horizontal displacement of the roller system and is a function of time t, m is equivalent mass of the roll, $c(x^2 - 1)$ represents nonlinear damping coefficient term between roller system and rolling piece, c is the nonlinear damping coefficient. $k_1 + k_2x^2$ represents nonlinear stiffness coefficient term between roller system and frame, and k_1 is the linear stiffness coefficient, k_2 is the nonlinear

stiffness coefficient. $D_t^q x$ is the q-order derivative of x with respect to time represents fractional derivative term, K is a positive coefficient. Due to the presence of friction, clearance, and additional bending moments, the roll system is subjected to a horizontal resultant force, which is defined as the horizontal excitation force $F\cos\omega t$, with the amplitude and frequency parameters F and ω, respectively. There are many definitions available for the fractional-order derivative, in this study, $D_t^q x$ with $0 \le q \le 1$ is the Caputo's fractional derivative of $x(t)$ described by

$$D_t^q x(t) = \frac{1}{\Gamma(1-q)} \int_0^t \dot{x}(s)(t-s)^{-q} ds,$$

in which $\Gamma(z)$ is Gamma function satisfying $\Gamma(z+1) = z\Gamma(z)$.

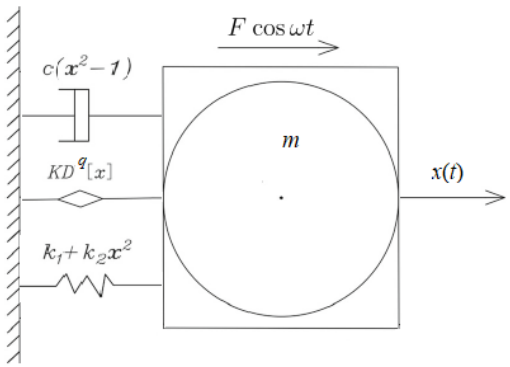

Figure 1. Physical model of horizontal vibration with fractional order.

The roll system of the rolling mill is a highly nonlinear hysteresis system. In the rolling process of composite plates, the elastic-plastic deformation process of the rolled piece is a nonlinear deformation process with time delay characteristics. The time-delay feedback control method is one of the effective methods for studying bifurcation control of nonlinear systems. We adopt time-delay feedback control to suppress the nonlinear vibration. The block diagram is shown in Figure 2.

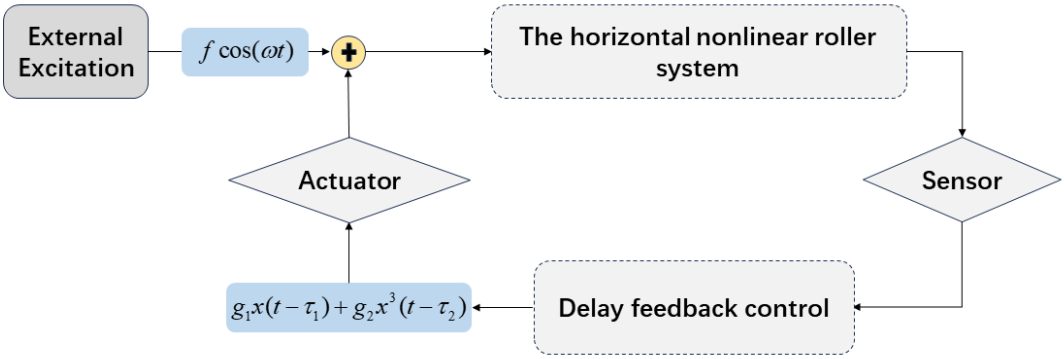

Figure 2. A block diagram of the time-delayed feedback control.

2.2. Multiple scale method

The horizontal vibration of the roller system is a weak vibration, and the multiple scale method can be used to conduct an approximate resonant solution of Eq (2.1), for which a small time scale parameter ε is required. This method begins by introducing new time variables $T_n = \varepsilon^n t, (n = 0, 1)$, then an approximate solution of Eq (2.1) with small amplitudes can be represented by

$$x = x_0(T_0, T_1) + \varepsilon x_1(T_0, T_1) + \cdots . \tag{2.2}$$

For such a small parameter ε, the following variable substitution is introduced for the system,

$$\varepsilon\mu = \frac{K}{m}, \quad \omega_0 = \sqrt{\frac{k_1}{m}}, \quad \varepsilon\alpha = \frac{c}{m}, \quad \varepsilon\beta = \frac{k_2}{m}, \quad f = \frac{F}{m}, \tag{2.3}$$

where ω_0 is the undamped natural frequency of the system, α, β, μ are equivalent nonlinear damping coefficient, equivalent fractional derivative coefficient and equivalent cubic stiffness coefficient, respectively.

Then, Eq (2.1) becomes

$$\ddot{x} + \omega_0^2 x + \varepsilon\mu D_t^q x + \varepsilon\alpha(x^2 - 1)\dot{x} + \varepsilon\beta x^3 = f\cos\omega t. \tag{2.4}$$

The derivatives with respect to t can be expressed in terms of the new scaled times T_n as a series of partial derivatives (see [16]),

$$\frac{\mathrm{d}}{\mathrm{d}t} = \frac{\partial}{\partial T_0}\frac{\mathrm{d}T_0}{\mathrm{d}t} + \frac{\partial}{\partial T_1}\frac{\mathrm{d}T_1}{\mathrm{d}t} + \cdots = D_0 + \varepsilon D_1 + \cdots , \tag{2.5a}$$

$$\frac{\mathrm{d}^2}{\mathrm{d}t^2} = D_0^2 + 2\varepsilon D_0 D_1 + \varepsilon^2 D_1^2 + \cdots , \tag{2.5b}$$

$$D_t^q = D_0^q + q\varepsilon D_0^{q-1} D_1 + \cdots , \tag{2.5c}$$

in which $D_0^q = \frac{\partial^q}{\partial T_0^q}$, $D_n = \frac{\partial}{\partial T_n}$, $D_n^2 = \frac{\partial^2}{\partial T_n^2}$, $(n = 0, 1)$.

3. Primary resonance and time-delay feedback control

The nonlinear vibration characteristics of the horizontal roller system may lead to various resonance phenomena during the rolling process, such as internal resonance, primary resonance, and secondary resonance. First, we analyze the primary resonance when the excitation frequency is close to the natural frequency.

3.1. Primary resonance

3.1.1. Amplitude-frequency response equation

Regarding the primary resonance, soft excitation is applied implying that the amplitude of excitation is small, thus the external force is given by

$$f \to \varepsilon f, \tag{3.1}$$

and the resonance relation is considered to be $\omega = \omega_0$ or $\omega \approx \omega_0$, a detuning parameter σ describing the nearness of ω to ω_0 is introduced by

$$\omega = \omega_0 + \varepsilon\sigma, \tag{3.2}$$

then $\omega t = \omega_0 T_0 + \sigma T_1$. Substituting (2.2), (2.5a)–(2.5c) into (2.4) leads to the following equation

$$\begin{aligned}&(D_0^2 + 2\varepsilon D_0 D_1 + \varepsilon^2 D_1^2)(x_0 + \varepsilon x_1) + \omega_0^2(x_0 + \varepsilon x_1) + \varepsilon\mu \cdot (D_0^q + q\varepsilon D_0^{q-1} D_1)(x_0 + \varepsilon x_1)\\ &+ \varepsilon\alpha[(x_0 + \varepsilon x_1)^2 - 1] \cdot (D_0 + \varepsilon D_1)(x_0 + \varepsilon x_1) + \varepsilon\beta(x_0 + \varepsilon x_1)^3\\ =&\varepsilon f \cos(\omega_0 T_0 + \sigma T_1).\end{aligned}$$

Equating the coefficients of the same power of ε, a set of linear differential equations are obtained:

$$O(\varepsilon^0) : D_0^2 x_0 + \omega_0^2 x_0 = 0, \tag{3.3}$$

$$O(\varepsilon^1) : D_0^2 x_1 + \omega_0^2 x_1 = -2D_0 D_1 x_0 - \mu D_0^q x_0 - \beta x_0^3 - \alpha(x_0^2 - 1) D_0 x_0 + f\cos(\omega_0 T_0 + \sigma T_1), \tag{3.4}$$

from which x_0 and x_1 can be solved one-by-one respectively. In this way, the resonant solution x is dominated by x_0, collected by εx_1.

The general solution of Eq (3.3) is of the form,

$$x_0 = A(T_1)\mathrm{e}^{\mathrm{i}\omega_0 T_0} + \overline{A}(T_1)\mathrm{e}^{-\mathrm{i}\omega_0 T_0}, \tag{3.5}$$

where $A(T_1)$ and $\overline{A}(T_1)$ are unknown functions, $\overline{A}(T_1)$ denotes the complex conjugate of $A(T_1)$.

To solve Eq (3.4), the qth-order ($0 \le q \le 1$) derivative of $\mathrm{e}^{\mathrm{i}\omega t}$ is approximated written as following (see [32]),

$$D_t^q \mathrm{e}^{\mathrm{i}\omega t} \approx (\mathrm{i}\omega)^q \mathrm{e}^{\mathrm{i}\omega t}. \tag{3.6}$$

Substituting (3.5) and (3.6) into Eq (3.4) and using

$$\cos(\omega_0 T_0 + \sigma T_1) = \frac{\mathrm{e}^{\mathrm{i}(\omega_0 T_0 + \sigma T_1)} + \mathrm{e}^{-\mathrm{i}(\omega_0 T_0 + \sigma T_1)}}{2},$$

the right-hand of Eq (3.4) becomes

$$[-2\mathrm{i}\omega_0 D_1 A - \mu A(\mathrm{i}\omega_0)^q - (3\beta + \mathrm{i}\omega_0\alpha)A^2\bar{A} + \mathrm{i}\omega_0\alpha A + \frac{f}{2}\mathrm{e}^{\mathrm{i}\sigma T_1}]\mathrm{e}^{\mathrm{i}\omega_0 T_0} + NST + cc, \tag{3.7}$$

where NST stands for the terms that do not produce secular terms, cc denotes the complex conjugate of the preceding terms.

In order that x_1 is periodic, the secular terms with $\mathrm{e}^{\mathrm{i}\omega_0 T_0}$ must be zero, namely

$$2\mathrm{i}\omega_0 D_1 A + \mu A(\mathrm{i}\omega_0)^q + (3\beta + \mathrm{i}\omega_0\alpha)A^2\bar{A} - \mathrm{i}\omega_0\alpha A - \frac{f}{2}\mathrm{e}^{\mathrm{i}\sigma T_1} = 0. \tag{3.8}$$

To solve Eq (3.8), we write $A(T_1)$ in the polar form as following

$$A(T_1) = \frac{a(T_1)}{2}\mathrm{e}^{\mathrm{i}\theta(T_1)}, \tag{3.9}$$

in which $a(T_1)$ and $\theta(T_1)$ are real functions of T_1.

With the help of the Euler formula

$$\mathrm{i}^q = (\mathrm{e}^{\mathrm{i}\pi/2})^q = \mathrm{e}^{\mathrm{i}q\pi/2} = \cos\frac{q\pi}{2} + \mathrm{i}\sin\frac{q\pi}{2}, \tag{3.10}$$

let $\varphi \overset{\text{def}}{=} \sigma T_1 - \theta$, by separating the real and imaginary parts of Eq (3.8), the differential equations governing amplitude $a(T_1)$ and $\varphi(T_1)$ of $A(T_1)$ are expressed as follows respectively

$$D_1 a = -\frac{\mu a}{2}\omega_0^{q-1}\sin\frac{q\pi}{2} + \frac{\alpha a}{2} - \frac{\alpha a^3}{8} + \frac{f}{2\omega_0}\sin\varphi, \tag{3.11a}$$

$$aD_1\varphi = \sigma a - \frac{\mu a}{2}\omega_0^{q-1}\cos\frac{q\pi}{2} - \frac{3\beta}{8\omega_0}a^3 + \frac{f}{2\omega_0}\cos\varphi. \tag{3.11b}$$

The steady state motions for the primary resonance response correspond to the fixed points of (3.11a) and (3.11b), that is, $D_1 a = 0$ and $D_1\varphi = 0$, namely

$$-\frac{\mu a}{2}\omega_0^{q-1}\sin\frac{q\pi}{2} + \frac{\alpha a}{2} - \frac{\alpha a^3}{8} = -\frac{f}{2\omega_0}\sin\varphi, \tag{3.12a}$$

$$\sigma a - \frac{\mu a}{2}\omega_0^{q-1}\cos\frac{q\pi}{2} - \frac{3\beta}{8\omega_0}a^3 = -\frac{f}{2\omega_0}\cos\varphi. \tag{3.12b}$$

By performing square operations and eliminating φ from Eqs (3.12a) and (3.12b), the following amplitude-frequency response equation is determined,

$$[(\frac{\mu}{2}\omega_0^{q-1}\sin\frac{q\pi}{2} - \frac{\alpha}{2} + \frac{\alpha}{8}a^2)^2 + (\sigma - \frac{\mu}{2}\omega_0^{q-1}\cos\frac{q\pi}{2} - \frac{3\beta}{8\omega_0}a^2)^2]a^2 = (\frac{f}{2\omega_0})^2. \tag{3.13}$$

The amplitude of the response is a function of external detuning parameter and the amplitude of excitation. It should be pointed out that in [26], the multiple scale method was used to obtain the amplitude-frequency response equation of Eq (2.1) for the primary resonance, but the coefficients in the expression were incorrect. In addition, when $\mu = 0$, Eq (2.4) is transformed into an integer-order model, and the corresponding amplitude-frequency response equation for the primary resonance has been studied in [13], but the expression has certain problems.

3.1.2. Stability of the steady resonant solutions

To determine the stability of steady state motion through the nature of singular points in Eqs (3.11a) and (3.11b), the following method can be used. Assume that $(a, \varphi) = (a^*, \varphi^*)$ is a steady solution of Eqs (3.11a) and (3.11b), let $\Delta a = a - a^*$ and $\Delta\varphi = \varphi - \varphi^*$. According to Eqs (3.12a) and (3.12b), the linearized differential equations governing Δa and $\Delta\varphi$ are

$$D_1\Delta a = -[\frac{\mu}{2}\omega_0^{q-1}\sin\frac{q\pi}{2} - \frac{\alpha}{2} + \frac{3\alpha(a^*)^2}{8}]\Delta a + \frac{f}{2\omega_0}\cos\varphi^*\,\Delta\varphi, \tag{3.14a}$$

$$D_1\Delta\varphi = [\frac{\sigma}{a^*} - \frac{\mu}{2a^*}\omega_0^{q-1}\cos\frac{q\pi}{2} - \frac{9\beta}{8\omega_0}a^*]\Delta a - \frac{f}{2\omega_0 a^*}\sin\varphi^*\,\Delta\varphi. \tag{3.14b}$$

Let $P = \frac{\mu}{2}\omega_0^{q-1}\sin\frac{q\pi}{2} - \frac{\alpha}{2} + \frac{3\alpha(a^*)^2}{8}$, $Q = \frac{\mu}{2}\omega_0^{q-1}\sin\frac{q\pi}{2} - \frac{\alpha}{2} + \frac{\alpha(a^*)^2}{8}$, $M = \sigma - \frac{\mu}{2}\omega_0^{q-1}\cos\frac{q\pi}{2} - \frac{3\beta}{8\omega_0}(a^*)^2$, $N = \sigma - \frac{\mu}{2}\omega_0^{q-1}\cos\frac{q\pi}{2} - \frac{9\beta}{8\omega_0}(a^*)^2$, then the characteristic equation can be rewritten as

$$\begin{vmatrix} -P-\lambda & -a^*M \\ \frac{1}{a^*}N & -Q-\lambda \end{vmatrix} = 0. \tag{3.15}$$

By expanding the determinant, one has

$$\lambda^2 + (P+Q)\lambda + (PQ+MN) = 0. \tag{3.16}$$

Consider when $P + Q > 0$, then the steady solution $(a, \varphi) = (a^*, \varphi^*)$ is asymptotically stable if and only if $\Lambda > 0$, where

$$\Lambda \stackrel{\text{def}}{=} PQ + MN. \tag{3.17}$$

3.1.3. Analysis of the resonant solutions

The influence of different parameters on the amplitude of resonance solution is investigated numerically, as shown in the Figures 3 and 4. With fixed parameter values, all the figures exhibit typical characteristics of hardening spring.

First, the influence of fractional order q on the resonant solutions is shown in Figure 3, where the parameters are selected to be, $\alpha = 0.04$, $\beta = 0.1$, $\omega_0 = 1$, $\mu = 0.02$ and $f = 0.1$. It can be seen that the smaller the order q is, the larger the maximum amplitude is. In addition, compared with the integer order case when $q = 1$, the bending degree, resonance peak, and resonance region of the amplitude-frequency curve of the fractional system change accordingly with the decrease of the fractional order q. The reason for this is that the fractional differential term has both stiffness and damping characteristics, which have a significant impact on the amplitude frequency response curve of the system. When the fractional-order q approaches 0, the fractional differential term is almost equivalent to the effect of linear stiffness; When q tends towards 1, the fractional differential term is almost equivalent to the effect of linear damping, and the larger the damping, the smaller the peak value.

Figure 4 presents parameter effect on resonant amplitudes with respect to μ, f, α and β. Here, the fractional-order $q = 0.9$ and the natural frequency $\omega_0 = 1$. In Figure 4(a), with the increase of μ, the nonlinear jump of the system weakens and the resonance amplitude of the system decreases. In other words, as μ increases, the unstable portions decrease. In Figure 4(b), with the increase of pulse pressure f, the nonlinear jump of the system is more obvious, and the resonance range and resonance amplitude of the system increase. In Figure 4(c), when the value of α increases, the amplitude of the system decreases. Since α is the nonlinear damping coefficient, increasing α means that the damping term increases, and the amplitude of resonance correspondingly decreases. In Figure 4(d), when the nonlinear stiffness coefficient β increases, the curve shifts to the right and and the degree of curvature increases. It can also be observed that the jumping phenomenon occur in the system, leading to system oscillations. Another phenomenon is that the amplitude does not change with the stiffness coefficient and remains consistent. According to the above analysis results, a controller should be designed to reduce the influence of primary resonance.

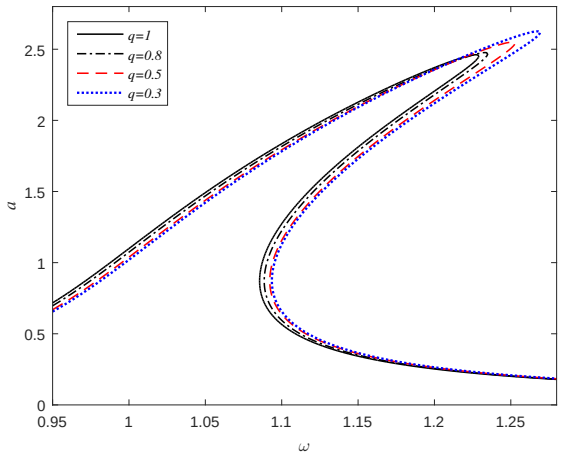

Figure 3. Effect of the fractional-order q on the amplitude-frequency curves.

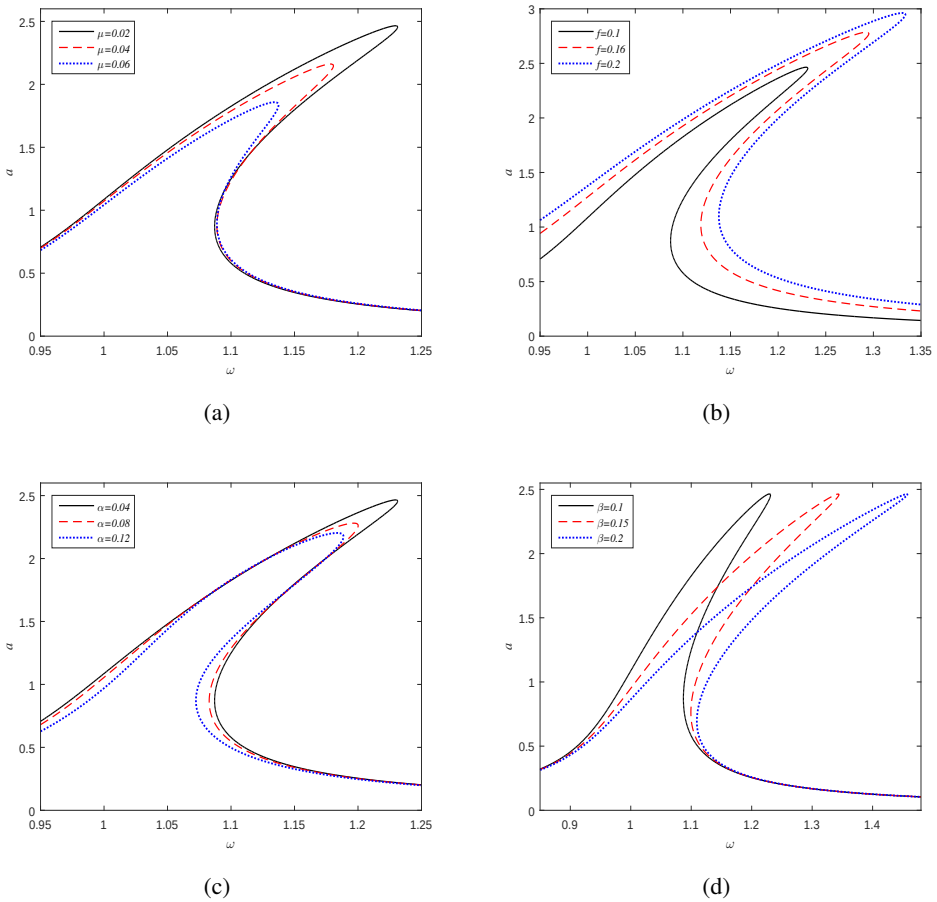

(a) (b)

(c) (d)

Figure 4. Parameter effect on the amplitude-frequency curves when (a) $\alpha = 0.04$, $\beta = 0.1$, $f = 0.1$, (b) $\alpha = 0.04$, $\beta = 0.1$, $\mu = 0.02$, (c) $\beta = 0.1$, $\mu = 0.02$, $f = 0.1$, (d) $\alpha = 0.04$, $\mu = 0.02$, $f = 0.1$.

3.2. Time-delay feedback control of primary resonance

3.2.1. Amplitude-frequency response equation

In order to eliminate the jumping and hysteresis phenomena of the primary resonance in the horizontal roller system, the time-delay displacement feedback strategy is adopted here, and the fractional equation with time-delay feedback control can be established as follows:

$$\ddot{x} + \omega_0^2 x + \varepsilon\mu D_t^q x + \varepsilon\alpha(x^2 - 1)\dot{x} + \varepsilon\beta x^3 = \varepsilon f\cos\omega t + \varepsilon g_1 x(t-\tau_1) + \varepsilon g_2 x^3(t-\tau_2), \tag{3.18}$$

where g_1 is the linear control gain, g_2 is the nonlinear control gain, τ_1 and τ_2 are time-delay parameters.

Substituting (2.2), (2.5a)–(2.5c) into (3.18) leads to the following equation

$$\begin{aligned}&(D_0^2 + 2\varepsilon D_0 D_1 + \varepsilon^2 D_1^2)(x_0 + \varepsilon x_1) + \omega_0^2(x_0 + \varepsilon x_1) + \varepsilon\mu\cdot(D_0^q + q\varepsilon D_0^{q-1} D_1)(x_0 + \varepsilon x_1)\\ &+ \varepsilon\alpha[(x_0 + \varepsilon x_1)^2 - 1]\cdot(D_0 + \varepsilon D_1)(x_0 + \varepsilon x_1) + \varepsilon\beta(x_0 + \varepsilon x_1)^3\\ =&\varepsilon f\cos(\omega_0 T_0 + \sigma T_1) + \varepsilon g_1 x_0(t-\tau_1) + \varepsilon g_2 x_0^3(t-\tau_2).\end{aligned}$$

Thus, a set of linear differential equations can be obtained:

$$O(\varepsilon^0): D_0^2 x_0 + \omega_0^2 x_0 = 0, \tag{3.19}$$

$$\begin{aligned}O(\varepsilon^1): D_0^2 x_1 + \omega_0^2 x_1 =& -2D_0 D_1 x_0 - \mu D_0^q x_0 - \beta x_0^3 - \alpha(x_0^2 - 1)D_0 x_0\\ &+ f\cos(\omega_0 T_0 + \sigma T_1) + g_1 x_0(T_0 - \tau_1) + g_2 x_0^3(T_0 - \tau_2).\end{aligned} \tag{3.20}$$

Assume that the general solution of Eq (3.19) is (3.5), substituting (3.5) into Eq (3.20), the right-hand of Eq (3.20) becomes

$$\begin{aligned}&[-2\mathrm{i}\omega_0 D_1 A - \mu A(\mathrm{i}\omega_0)^q - (3\beta + \mathrm{i}\omega_0\alpha)A^2\bar{A} + \mathrm{i}\omega_0\alpha A + \frac{f}{2}\mathrm{e}^{\mathrm{i}\sigma T_1}\\ &+ g_1 A\mathrm{e}^{-\mathrm{i}\omega_0\tau_1} + 3g_2 A^2\bar{A}\mathrm{e}^{-\mathrm{i}\omega_0\tau_2}]\mathrm{e}^{\mathrm{i}\omega_0 T_0} + NST + cc,\end{aligned} \tag{3.21}$$

where NST stands for the terms that do not produce secular terms, cc denotes the complex conjugate of the preceding terms.

Through setting the coefficient of $\mathrm{e}^{\mathrm{i}\omega_0 T_0}$ equal to zero to eliminate the secular terms, the following equation can be obtained as:

$$2\mathrm{i}\omega_0 D_1 A + \mu A(\mathrm{i}\omega_0)^q + (3\beta + \mathrm{i}\omega_0\alpha)A^2\bar{A} - \mathrm{i}\omega_0\alpha A - \frac{f}{2}\mathrm{e}^{\mathrm{i}\sigma T_1} - g_1 A\mathrm{e}^{-\mathrm{i}\omega_0\tau} - 3g_2 A^2\bar{A}\mathrm{e}^{-\mathrm{i}\omega_0\tau_2} = 0. \tag{3.22}$$

Similar to the previous discussion, the following differential equations about amplitude and phase can be obtained,

$$D_1 a = -\frac{\mu a}{2}\omega_0^{q-1}\sin\frac{q\pi}{2} + \frac{\alpha a}{2} - \frac{\alpha a^3}{8} - \frac{g_1 a}{2\omega_0}\sin(\omega_0\tau_1) - \frac{3g_2 a^3}{8\omega_0}\sin(\omega_0\tau_2) + \frac{f}{2\omega_0}\sin\varphi, \tag{3.23a}$$

$$aD_1\varphi = \sigma a - \frac{\mu a}{2}\omega_0^{q-1}\cos\frac{q\pi}{2} - \frac{3\beta a^3}{8\omega_0} + \frac{g_1 a}{2\omega_0}\cos(\omega_0\tau_1) + \frac{3g_2 a^3}{8\omega_0}\cos(\omega_0\tau_2) + \frac{f}{2\omega_0}\cos\varphi. \tag{3.23b}$$

The steady state motions for the primary resonance response correspond to the fixed points of (3.23a) and (3.23b), that is, $D_1 a = 0$ and $D_1 \varphi = 0$, namely

$$-\frac{\mu a}{2}\omega_0^{q-1}\sin\frac{q\pi}{2} + \frac{\alpha a}{2} - \frac{\alpha a^3}{8} - \frac{g_1 a}{2\omega_0}\sin(\omega_0\tau_1) - \frac{3g_2 a^3}{8\omega_0}\sin(\omega_0\tau_2) = -\frac{f}{2\omega_0}\sin\varphi, \tag{3.24a}$$

$$\sigma a - \frac{\mu a}{2}\omega_0^{q-1}\cos\frac{q\pi}{2} - \frac{3\beta a^3}{8\omega_0} + \frac{g_1 a}{2\omega_0}\cos(\omega_0\tau_1) + \frac{3g_2 a^3}{8\omega_0}\cos(\omega_0\tau_2) = -\frac{f}{2\omega_0}\cos\varphi. \tag{3.24b}$$

The amplitude-frequency response equation of primary resonance with time-delay control can be obtained as:

$$[(\frac{1}{2}\mu_e + \frac{\alpha_e}{8}a^2)^2 + (\sigma_e - \frac{3\beta_e}{8\omega_0}a^2)^2]a^2 = (\frac{f}{2\omega_0})^2, \tag{3.25}$$

in which

$$\mu_e = \mu\omega_0^{q-1}\sin\frac{q\pi}{2} + \frac{g_1}{\omega_0}\sin(\omega_0\tau_1) - \alpha, \quad \alpha_e = \alpha + \frac{3g_2}{\omega_0}\sin(\omega_0\tau_2),$$

$$\sigma_e = \sigma - \frac{\mu}{2}\omega_0^{q-1}\cos\frac{q\pi}{2} + \frac{g_1}{2\omega_0}\cos(\omega_0\tau_1), \quad \beta_e = \beta - g_2\cos(\omega_0\tau_2).$$

From Eq (3.25), it can be seen that the amplitude of the response is a function of external detuning parameter, feedback gain, time delay and the amplitude of excitation.

3.2.2. Numerical simulation

The impact of adding time-delay feedback control on the amplitude-frequency response curve of the primary resonance is presented through numerical simulation, as shown in Figure 5. In Figure 5, the primary resonance amplitude and resonance region can be controlled, the primary resonance bifurcations can be reduced by properly adjusting the delay parameters (τ_1, τ_2) and feedback gains (g_1, g_2). After adding time-delay feedback control, the resonance peak value decreases, the curvature of the curve also decreases and the jumping phenomenon has also weakened. It can also be seen from Figure 5(a) that the control effect of simultaneously adjusting delay parameters (τ_1, τ_2) and feedback gains (g_1, g_2) is better than that of separately adjusting linear feedback gain g_1 or nonlinear feedback gain g_2.

In Figure 5(b), as the linear gain g_1 and nonlinear gain g_2 gradually increase, the amplitude of the primary resonance of the system gradually decreases, and the jumping phenomenon of the curve is eliminated. Therefore, it can be seen that when using only feedback control gain as the control parameter, if both linear and nonlinear feedback control gains increase simultaneously, the primary resonance phenomenon of the system can be reasonably controlled. In Figure 5(c), as the delay parameters (τ_1, τ_2) gradually increase, the amplitude and the resonance domain of the system gradually decreases. However, the adjustment of delay parameters has little effect on the degree of curve curvature. On the contrary, by adjusting the feedback control gains g_1 and g_2, it is relatively easy to eliminate the jumping phenomenon of the primary resonance. This indicates that using feedback control gain as the control object has a better control effect than using delay parameters as the control object.

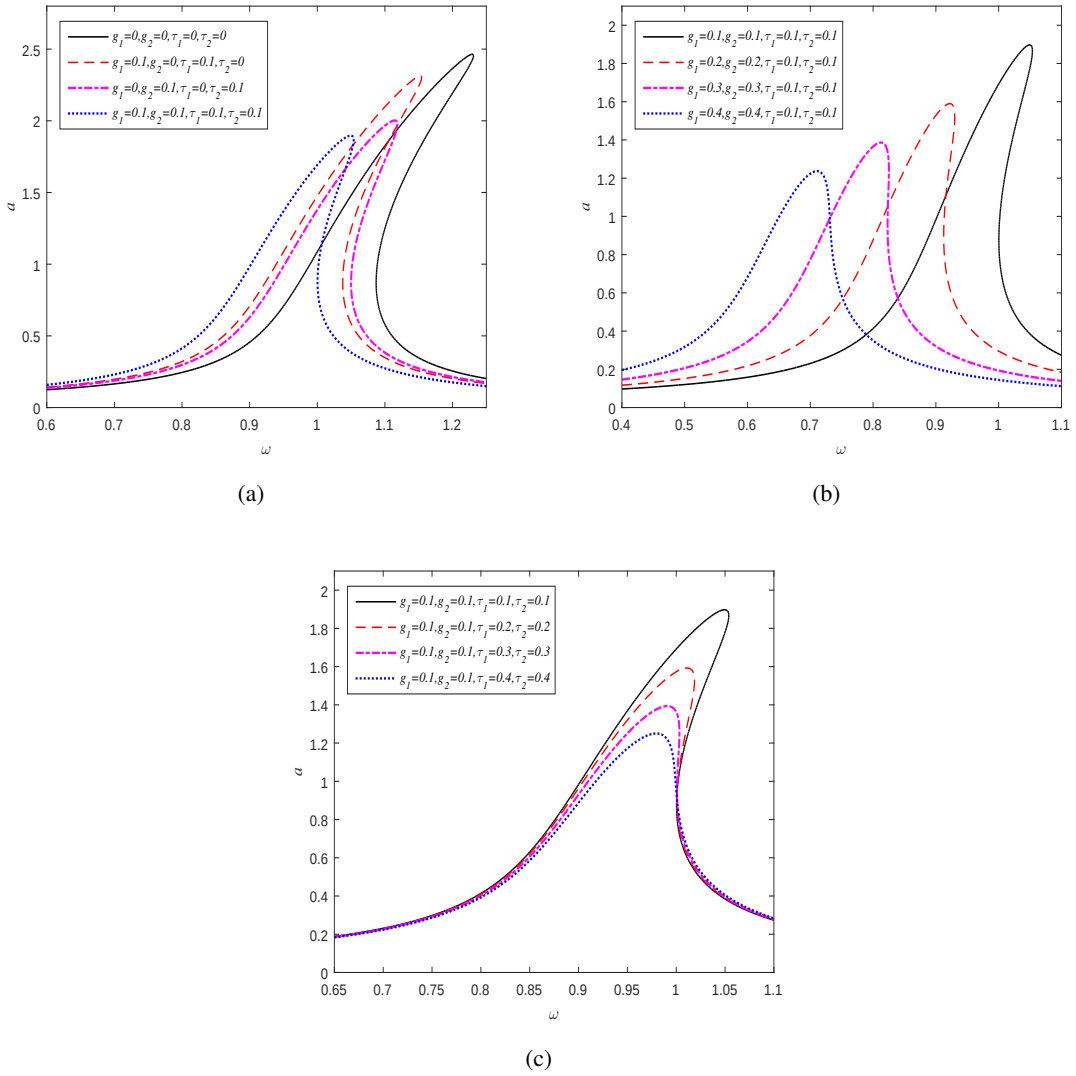

Figure 5. Effect of time-delay feedback control on the amplitude-frequency response curve of the primary resonance.

4. Secondary resonance and time-delay feedback control

In this section, we will discuss secondary resonance, namely superharmonic and subharmonic resonance. Only superharmonic resonance is considered here, and the issue of subharmonic resonance will be studied in subsequent papers.

4.1. Third-order superharmonic resonance

4.1.1. Amplitude-frequency response equation

During the inspection process of third-order superharmonic resonance, when the excitation frequency is far away from the natural frequency, unless its amplitude is sufficiently large, the impact

of excitation is minimal. Therefore, in superharmonic resonance, the excitation amplitude is of order ε^0. Third-order superharmonic resonance with limited amplitude occurs in the Eq (2.4) when $3\omega = \omega_0$ or $3\omega \approx \omega_0$, the resonance relation is represented as

$$3\omega = \omega_0 + \varepsilon\sigma, \tag{4.1}$$

in which σ is again the detuning parameter, then $3\omega T_0 = \omega_0 T_0 + \sigma T_1$. The following derivations in this section are similar to those in the previous section, only the main steps will be retained for ease of reading.

Substituting (4.1), (2.5a)–(2.5c) into (2.4) leads to the following equation

$$\begin{aligned}&(D_0^2 + 2\varepsilon D_0 D_1 + \varepsilon^2 D_1^2)(x_0 + \varepsilon x_1) + \omega_0^2(x_0 + \varepsilon x_1) + \varepsilon\mu \cdot (D_0^q + q\varepsilon D_0^{q-1} D_1)(x_0 + \varepsilon x_1)\\ &+ \varepsilon\alpha[(x_0 + \varepsilon x_1)^2 - 1] \cdot (D_0 + \varepsilon D_1)(x_0 + \varepsilon x_1) + \varepsilon\beta(x_0 + \varepsilon x_1)^3\\ =&f\cos(\omega T_0).\end{aligned}$$

Equating the coefficients of the same power of ε, a set of linear differential equations are obtained:

$$O(\varepsilon^0) : D_0^2 x_0 + \omega_0^2 x_0 = f\cos(\omega T_0), \tag{4.2}$$

$$O(\varepsilon^1) : D_0^2 x_1 + \omega_0^2 x_1 = -2D_0 D_1 x_0 - \mu D_0^q x_0 - \beta x_0^3 - \alpha(x_0^2 - 1)D_0 x_0. \tag{4.3}$$

The general solution of Eq (4.2) is of the following form,

$$x_0 = A(T_1)\mathrm{e}^{\mathrm{i}\omega_0 T_0} + \overline{A}(T_1)\mathrm{e}^{-\mathrm{i}\omega_0 T_0} + B(\mathrm{e}^{i\omega T_0} + \mathrm{e}^{-i\omega T_0}), \tag{4.4}$$

where $A(T_1)$ and $\overline{A}(T_1)$ are complex functions in terms of slow time scale, $\overline{A}(T_1)$ denotes the complex conjugate of $A(T_1)$ and $B = \frac{f}{2(\omega_0^2 - \omega^2)}$.

Substituting (4.4) into Eq (4.3), the right-hand of Eq (4.3) becomes

$$\begin{aligned}&[-2\mathrm{i}\omega_0 D_1 A - \mu A(\mathrm{i}\omega_0)^q - (3A^2\bar{A} + 6AB^2 + B^3\mathrm{e}^{\mathrm{i}\sigma T_1})\beta - (A^2\bar{A} + 2AB^2 - A)\mathrm{i}\omega_0\alpha\\ &- \alpha i\omega B^3\mathrm{e}^{\mathrm{i}\sigma T_1}]\mathrm{e}^{\mathrm{i}\omega_0 T_0} + NST + cc,\end{aligned} \tag{4.5}$$

where NST stands for the terms that do not produce secular terms, cc denotes the complex conjugate of the preceding terms.

Thus, the solvability condition takes the form

$$2\mathrm{i}\omega_0 D_1 A + \mu A(\mathrm{i}\omega_0)^q + (3A^2\bar{A} + 6AB^2)\beta + (A^2\bar{A} + 2AB^2 - A)\mathrm{i}\omega_0\alpha = -(\beta + \alpha i\omega)B^3\mathrm{e}^{\mathrm{i}\sigma T_1}. \tag{4.6}$$

Separating the real and imaginary parts, and letting $\varphi \overset{\text{def}}{=} \sigma T_1 - \theta$ to transform this into an autonomous system. Seeking the steady state, we let $D_1 a = 0$ and $D_1\varphi = 0$. Eliminating φ leads to the nonlinear the amplitude-frequency equation

$$[(\frac{\mu}{2}\omega_0^{q-1}\sin\frac{q\pi}{2} - \frac{4 - a^2 - 8B^2}{8}\alpha)^2 + (\sigma - \frac{\mu}{2}\omega_0^{q-1}\cos\frac{q\pi}{2} - \frac{3(a^2 + 8B^2)}{8\omega_0}\beta)^2]a^2 = \frac{(\beta^2 + \alpha^2\omega^2)B^6}{\omega_0^2}. \tag{4.7}$$

From Eq (4.7), it can be concluded that there is an interaction between the nonlinear term and the external force term to the third-order superharmonic resonance of the first-order perturbation analysis. According to Eq (4.7), different superharmonic resonance amplitude-frequency characteristic curves can be obtained by different μ, α, β, and f.

4.1.2. Numerical simulation

First, we present an image of the amplitude-frequency response curve of third-order superharmonic resonance, as shown in Figure 6. Here, the parameters are selected to be, $q = 0.9$, $\alpha = 0.08$, $\beta = 0.2$, $\omega_0 = 1$, $\mu = 0.08$, and $f = 0.24$. It can be clearly seen from Figure 6 that the fractional roller system generates superharmonic resonance under the above parameter conditions.

By changing the nonlinear damping coefficient α, nonlinear stiffness coefficient β, rolling force amplitude f, and fractional damping coefficient μ of the roller system, the superharmonic resonance curves with different amplitude-frequency characteristics can be obtained, as shown in Figure 7. Here, the fractional order $q = 0.9$ and the natural frequency $\omega_0 = 1$. In Figure 7(a), when the nonlinear damping coefficient α increases, the amplitude decreases and the resonance domain decreases. In Figure 7(b), with the nonlinear stiffness coefficient β increases, the curve shifts to the right and the bending degree increases. In Figure 7(c), with the increase of rolling force, the amplitude and resonance region of the system increase obviously. In Figure 7(d), when μ increases, the amplitude and the resonance domain decrease, and the nonlinear jump of the system weakens.

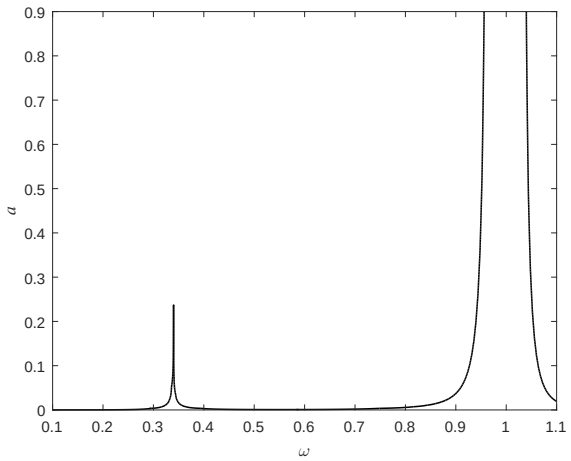

Figure 6. The amplitude-frequency response curve of third-order superharmonic resonance.

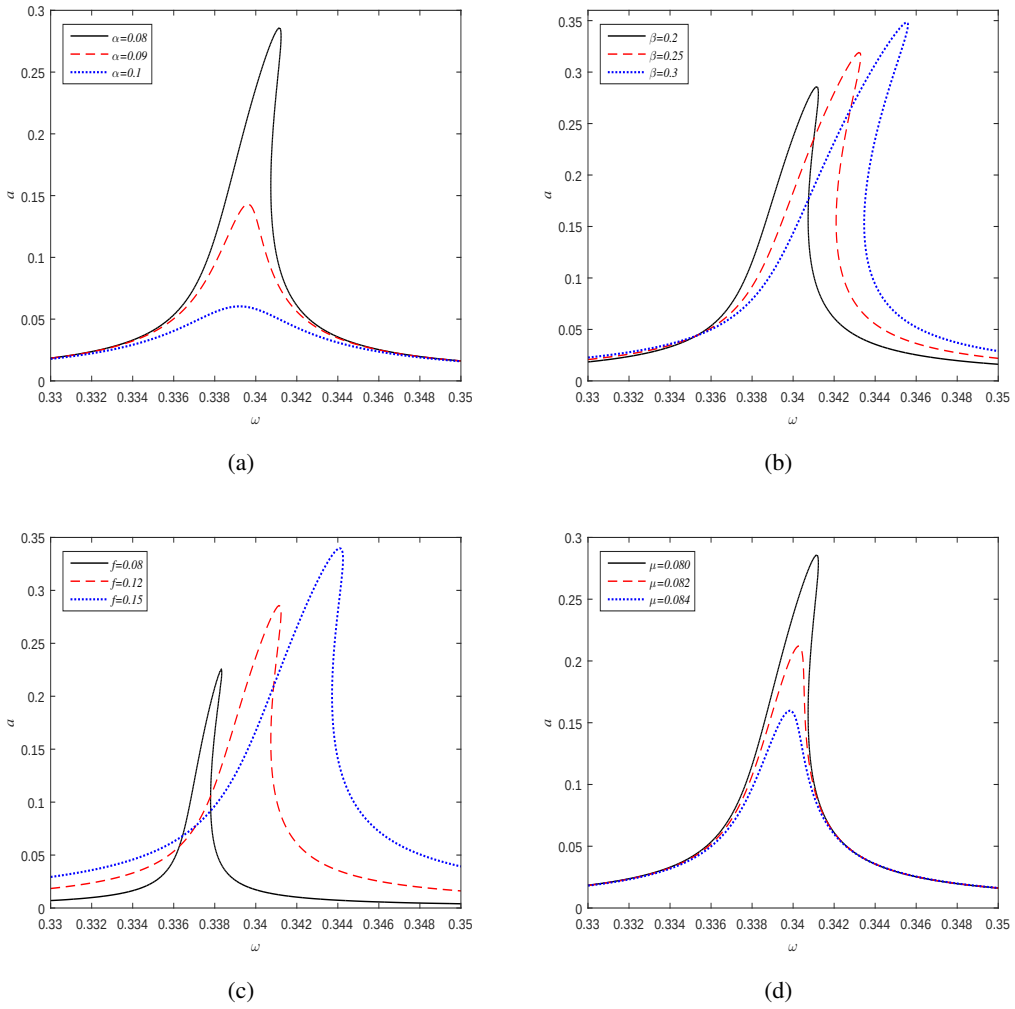

Figure 7. Parameter effect on the amplitude-frequency curves of third-order superharmonic resonance when (a) $\beta = 0.2$, $\mu = 0.08$, $f = 0.24$, (b) $\alpha = 0.08$, $\mu = 0.08$, $f = 0.24$, (c) $\alpha = 0.08, \beta = 0.2, \mu = 0.08$, (d) $\alpha = 0.08, \beta = 0.2, f = 0.24$.

4.2. Time-delay feedback control of superharmonic resonance

4.2.1. Amplitude-frequency response equation

In order to study the control problem of superharmonic resonance, the fractional equation with time-delay feedback control can be established as follows:

$$\ddot{x} + \omega_0^2 x + \varepsilon\mu D_t^q x + \varepsilon\alpha(x^2 - 1)\dot{x} + \varepsilon\beta x^3 = f\cos\omega t + \varepsilon g_1 x(t - \tau_1) + \varepsilon g_2 x^3(t - \tau_2). \tag{4.8}$$

Substituting (4.1), (2.5a)–(2.5c) into (4.8), we can obtain

$$\begin{aligned}&(D_0^2 + 2\varepsilon D_0 D_1 + \varepsilon^2 D_1^2)(x_0 + \varepsilon x_1) + \omega_0^2(x_0 + \varepsilon x_1) + \varepsilon\mu \cdot (D_0^q + q\varepsilon D_0^{q-1} D_1)(x_0 + \varepsilon x_1)\\ &+ \varepsilon\alpha[(x_0 + \varepsilon x_1)^2 - 1] \cdot (D_0 + \varepsilon D_1)(x_0 + \varepsilon x_1) + \varepsilon\beta(x_0 + \varepsilon x_1)^3\\ =&f\cos(\omega T_0) + g_1 x_0(T_0 - \tau_1) + g_2 x_0^3(T_0 - \tau_2).\end{aligned}$$

Equating the coefficients of the same power of ε, a set of linear differential equations are obtained:

$$O(\varepsilon^0) : D_0^2 x_0 + \omega_0^2 x_0 = f\cos(\omega T_0), \tag{4.9}$$

$$O(\varepsilon^1) : D_0^2 x_1 + \omega_0^2 x_1 = -2D_0 D_1 x_0 - \mu D_0^q x_0 - \beta x_0^3 - \alpha(x_0^2 - 1)D_0 x_0 + g_1 x_0(t-\tau_1) + g_2 x_0^3(t-\tau_2). \tag{4.10}$$

Assume that the solution of the zeroth approximation equation (4.9) is (4.4), substituting (4.4) into Eq (4.10), the right-hand of Eq (4.10) becomes

$$\begin{aligned}&[-2\mathrm{i}\omega_0 D_1 A - \mu A(\mathrm{i}\omega_0)^q - (3A^2\bar{A} + 6AB^2 + B^3\mathrm{e}^{\mathrm{i}\sigma T_1})\beta - (A^2\bar{A} + 2AB^2 - A)\mathrm{i}\omega_0\alpha \\ &- \alpha i\omega B^3\mathrm{e}^{\mathrm{i}\sigma T_1} + g_1 A\mathrm{e}^{-\mathrm{i}\omega_0\tau_1} + 3g_2 A^2\bar{A}\mathrm{e}^{-\mathrm{i}\omega_0\tau_2}]\mathrm{e}^{\mathrm{i}\omega_0 T_0} + NST + cc,\end{aligned} \tag{4.11}$$

where NST stands for the terms that do not produce secular terms, cc denotes the complex conjugate of the preceding terms.

The solvability condition takes the form

$$\begin{aligned}&2\mathrm{i}\omega_0 D_1 A + \mu A(\mathrm{i}\omega_0)^q + (3A^2\bar{A} + 6AB^2 + B^3\mathrm{e}^{\mathrm{i}\sigma T_1})\beta + (A^2\bar{A} + 2AB^2 - A)\mathrm{i}\omega_0\alpha \\ &+ \alpha i\omega B^3\mathrm{e}^{\mathrm{i}\sigma T_1} - g_1 A\mathrm{e}^{-\mathrm{i}\omega_0\tau_1} - 3g_2 A^2\bar{A}\mathrm{e}^{-\mathrm{i}\omega_0\tau_2} = 0.\end{aligned} \tag{4.12}$$

Based on the condition of steady solution, the nonlinear amplitude-frequency equation of superharmonic vibration with time-delay control can be obtained as follows

$$[(\frac{1}{2}\mu_s + \frac{\alpha_s}{8}a^2)^2 + (\sigma_s - \frac{3\beta_s}{8\omega_0}a^2)^2]a^2 = \frac{(\beta^2 + \alpha^2\omega^2)B^6}{\omega_0^2}, \tag{4.13}$$

in which

$$\mu_s = \mu\omega_0^{q-1}\sin\frac{q\pi}{2} + \frac{g_1}{\omega_0}\sin(\omega_0\tau_1) - \alpha + 2B^2\alpha, \quad \alpha_s = \alpha + \frac{3g_2}{\omega_0}\sin(\omega_0\tau_2),$$

$$\sigma_s = \sigma - \frac{\mu}{2}\omega_0^{q-1}\cos\frac{q\pi}{2} + \frac{g_1}{2\omega_0}\cos(\omega_0\tau_1) - \frac{3B^2\beta}{\omega_0}, \quad \beta_s = \beta - \frac{g_2}{\omega_0}\cos(\omega_0\tau_2).$$

From Eq (4.13), it can be concluded that there is an interaction between the feedback gain, time delay, nonlinear term and the external force term to the third-order superharmonic resonance of the first-order perturbation analysis.

4.2.2. Numerical simulation

The impact of adding time-delay feedback control on the amplitude-frequency response curve of the third-order superharmonic resonance is presented through numerical simulation, as shown in Figure 8. Figure 8 shows that the amplitude and resonance region can be controlled and the superharmonic resonance bifurcations can be reduced by properly adjusting the delay parameters (τ_1, τ_2) and feedback gains (g_1, g_2). After adding time-delay feedback control, the resonance peak value decreases, the curvature of the curve decreases, and the jumping phenomenon has weakened.

In Figure 8(a), as the feedback gains (g_1, g_2) gradually increase, the amplitude of the system gradually decreases, the resonance domain gradually decreases, and the curve bifurcation is eliminated. The resonance domain also shows significant movement. It can be concluded that using feedback

control gain as the control parameter and increasing both linear and nonlinear feedback control gains can effectively control the phenomenon of superharmonic vibration in the system. In Figure 8(b), when the delay parameters (τ_1, τ_2) gradually increases, the amplitude of the system gradually decreases and the resonance domain gradually decreases. Through comparison, it can be found that whether using feedback control gains or time-delay parameters as the control object, the control effect is significant during the control of superharmonic vibration.

At the end of this section, a time history diagram is used to briefly illustrate the impact of feedback control on the model. Figure 9 shows the time history of the superharmonic resonance under feedback control. The various parameters of the system in Figure 9 are $q = 0.9$, $\omega_0 = 1$, $\alpha = 0.08$, $\beta = 0.2$, $\mu = 0.08$, and $f = 0.24$. It can be observed that the amplitude of the resonance decreases obviously after the delay control is added, and the larger the delay is, the greater the amplitude reduction is.

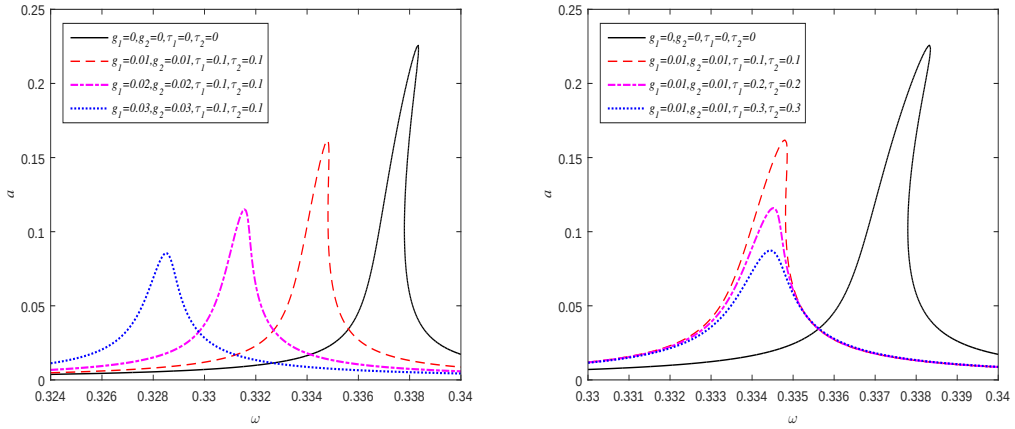

(a) (b)

Figure 8. Effect of time-delay feedback control on the amplitude-frequency response curve of the third-order superharmonic resonance.

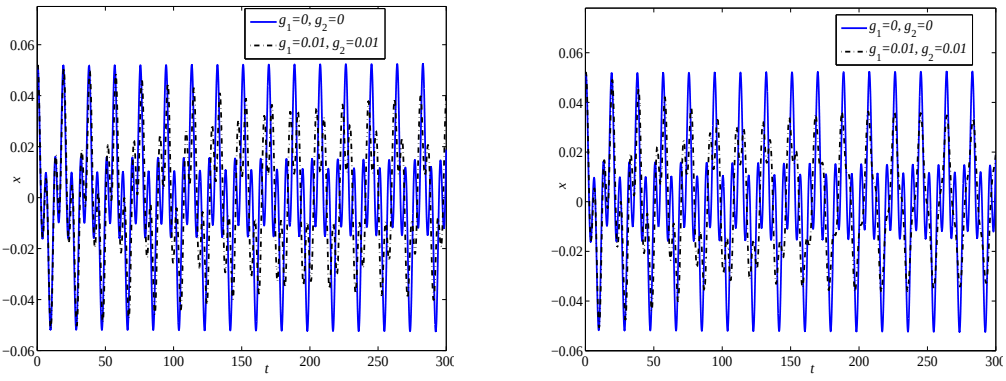

(a) (b)

Figure 9. The time history of the superharmonic resonance under feedback control for (a) $\tau = 0.01$, (b) $\tau = 0.02$.

5. Comparison between approximate analytical solution and numerical solution

According to Eq (3.13), the primary resonance amplitude-frequency response curve of the system can be drawn. For comparison, we adopt the power series method introduced in reference [33, 34], and its calculation formula is

$$D_{t_n}^q[y(t_n)] \approx h^{-q} \sum_{j=0}^{n} C_j^q y(t_{n-j}), \tag{5.1}$$

where $t_n = nh$ is the sample points, h is the sample step, and C_j^q is the fractional binomial coefficient with the iterative relationship as

$$C_0^q = 1, \quad C_j^q = (1 - \frac{1+q}{j})C_{j-1}^q. \tag{5.2}$$

According to Eqs (5.1) and (5.2), the numerical scheme for Eq (2.4) can be expressed as

$$x(t_n) = y(t_{n-1})h - \sum_{j=1}^{n} C_j^1 x(t_{n-j}), \tag{5.3a}$$

$$y(t_n) = \{f\cos(\omega t_n) - \lambda x(t_n) - \beta x^3(t_n) + \alpha[1 - x^2(t_n)]x(t_{n-1}) - \mu z(t_{n-1})\}h - \sum_{j=1}^{n} C_j^1 y(t_{n-j}), \tag{5.3b}$$

$$z(t_n) = y(t_n)h^{1-q} - \sum_{j=1}^{n} C_j^{1-q} z(t_{n-j}). \tag{5.3c}$$

The numerical amplitude-frequency curve marked with circle in Figure 10, where the stepsize of time is $h = 0.005$, and the total computation time is 100s with the first 25s neglected. It shows that the resonant amplitude calculated from Eq (3.13) is in good agreement with the numerical results, especially when the $\omega \approx \omega_0$.

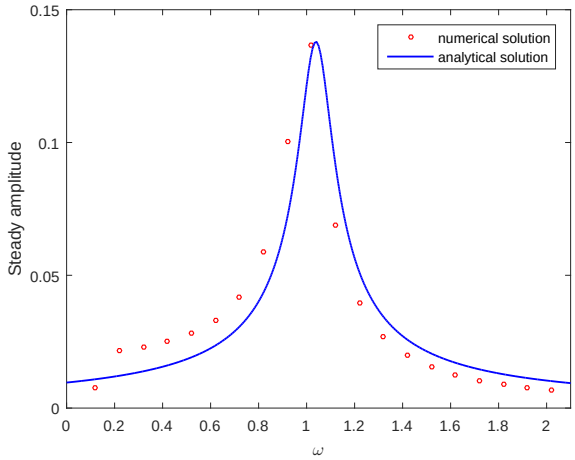

Figure 10. Comparison between approximate analytical solution and numerical solution when $\omega_0 = 1$, $q = 0.75$, $\mu = 0.2$, $\alpha = 0.04$, $\beta = 0.1$, $f = 0.02$.

6. Conclusions

In the present research, we study the nonlinear vibration characteristics and time-delay feedback controllability of a fractional horizontal roll systems for rolling mill, described by a damped fractional Duffing-van der Pol oscillator under external harmonic excitation. In response to the inaccurate conclusions in existing literature, we conducted rigorous derivation. The accurate amplitude-frequency response equations were obtained by the multiple scale method. The influence of parameters on system characteristics was studied using amplitude frequency response equation. Furthermore, the time-delay feedback controller is designed to control the parameter excitation vibration. The numerical simulation results verified the effectiveness of the time-delay controller in eliminating the jumping and hysteresis phenomena of the rolling system. It can also be concluded that fractional order and the damping coefficient are very important in fractional horizontal roll systems. For example, a larger fractional order and larger damping coefficient can reduce the effective amplitude of resonance and change the resonance frequency.

Through the study of the roll model, it is inspired that in the design process of strip rolling mills, the influence of rolling force amplitude on primary resonance and superharmonic resonance should be avoided and reduced. Further research is needed to combine active vibration control techniques such as PID control, adaptive control, fuzzy control, and other control methods to analyze the vibration control effect of the rolling mill.

Author contributions

Zhoujin Cui performed the conceptualization, methodology, writing-original draft and writing-review & editing; Xiaorong Zhang performed the investigation and validation; Tao Lu performed the validation and supervision. All authors have read and approved the final version of the manuscript for publication.

Use of AI tools declaration

The authors declare they have not used Artificial Intelligence (AI) tools in the creation of this article.

Acknowledgments

The authors express gratitude to the reviewers and editors for their helpful comments and suggestions, as well as to the financial support from High Level Talent Research Launch Fund of Jiangsu Second Normal University (No. 928201/058).

Conflict of interest

All authors declare no conflicts of interest in this paper.

References

1. C. W. Knight, S. J. Hardy, A. W. Lees, K. J. Brown, Investigations into the influence of asymmetric factors and rolling parameters on strip curvature during hot rolling, *J. Mater. Process. Tech.*, **134** (2003), 180–189. https://doi.org/10.1016/S0924-0136(02)00469-7
2. D. He, T. Wang, Z. Ren, G. Feng, Y. Liu, Principal resonance time-delay feedback control of roller system in corrugated rolling mills, (In chinese), *Control Theory Technol.*, **37** (2020), 1552–1561. https://doi.org/10.7641/CTA.2020.90367
3. S. Kapil, P. Eberhard, S. K. Dwivedy, Nonlinear dynamic analysis of a parametrically excited cold rolling mill, *J. Manuf. Sci. Eng.*, **136** (2014), 041012. https://doi.org/10.1115/1.4026961
4. R. Peng, X. Zhang, P. Shi, Vertical-horizontal coupling vibration of hot rolling mill rolls under multi-piecewise nonlinear constraints, *Metals*, **11** (2021), 170. https://doi.org/10.3390/met11010170
5. M. A. Younes, M. Shahtout, M. N. Damir, A parameters design approach to improve product quality and equipment performance in hot rolling, *J. Mater. Process. Tech.*, **171** (2006), 83–92. https://doi.org/10.1016/j.jmatprotec.2005.06.052
6. J. Sun, Y. Peng, H. Liu, Non-Linear vibration and stability of moving strip with time-dependent tension in rolling process, *J. Iron Steel Res. Int.*, **17** (2010), 11–20. https://doi.org/10.1016/S1006-706X(10)60106-9
7. X. Fan, Y. Zang, H. Wang, Research on vertical vibration of hot rolling mill, (In chinese), *China Mech. Eng.*, **21** (2010), 1801–1804.
8. X. Fan, Y. Zang, Y. Sun, P. Wang, Impact analysis of roller system stability for four-high mill horizontal vibration, *Shock Vib.*, **2016** (2016), 5693584. https://doi.org/10.1155/2016/5693584
9. P. Shi, J. Li, J. Jiang, B. Liu, D. Han, Nonlinear dynamics of torsional vibration for rolling mill's main drive system under parametric excitation, *J. Iron Steel Res. Int.*, **20** (2013), 7–12. https://doi.org/10.1016/S1006-706X(13)60037-0
10. Y. Kimura, N. Fujita, Y. Matsubara, K. Kobayashi, Y. Amanuma, O. Yoshiokai, et al., High-speed rolling by hybrid-lubrication system in tandem cold rolling mills, *J. Mater. Process. Technol.*, **216** (2015), 357–368. https://doi.org/10.1016/j.jmatprotec.2014.10.002
11. X. Yang, C. Tong, Nonlinear modeling and global sliding mode control of main drive system torsional vibration in cold rollling mill, In: *2012 Fifth international conference on intelligent computation technology and automation*, 2012, 233–236. https://doi.org/10.1109/ICICTA.2012.65
12. B. Liu, J. Jiang, K. Wang, P. Li, G. Pan, Roll system vibration control of rolling mill based on time delay feedback, *Mechatron. Manuf. Technol.*, 2017, 260–265. https://doi.org/10.1142/9789813222359_0035
13. D. He, H. Xu, T. Wang, Z. Ren, Nonlinear time-delay feedback controllability for vertical parametrically excited vibration of roll system in corrugated rolling mill, *Metall. Res. Technol.*, **117** (2020), 210. https://doi.org/10.1051/metal/2020020
14. A. P. Singh, D. Deb, H. Agrawal, K. Bingi, S. Ozana, Modeling and control of robotic manipulators: A fractional calculus point of view, *Arab. J. Sci. Eng.*, **46** (2021), 9541–9552. https://doi.org/10.1007/s13369-020-05138-6

15. E. Viera-Martin, J. F. Gómez-Aguilar, J. E. Solís-Pérez, J. A. Hernández-Pérez, R. F. Escobar-Jiménez, Artificial neural networks: A practical review of applications involving fractional calculus, *Eur. Phys. J. Spec. Top.*, **231** (2022), 2059–2095. https://doi.org/10.1140/epjs/s11734-022-00455-3

16. Z. Cui, Z. Wang, Primary resonance of a nonlinear fractional model for cerebral aneurysm at the circle of Willis, *Nonlinear Dyn.*, **108** (2022), 4301–4314. http://dx.doi.org/10.1007/s11071-022-07445-z

17. Z. Cui, Solutions of some typical nonlinear differential equations with Caputo-Fabrizio fractional derivative, *AIMS Mathematics*, **7** (2022), 14139–14153. https://doi.org/10.3934/math.2022779

18. K. A. Lazopoulos, Stability criteria and Λ-fractional mechanics, *Fractal Fract.*, **7** (2023), 248. https://doi.org/10.3390/fractalfract7030248

19. J. Liu, H. Tian, Z. Wang, Y. Guan, Z. Cao, Dynamical analysis and misalignment projection synchronization of a novel RLCM fractional-order memristor circuit system, *Axioms*, **12** (2023), 1125. https://doi.org/10.3390/axioms12121125

20. Z. Li, Z. Zhang, Stabilization control for a class of fractional-order HIV-1 infection model with time delays, *Axioms*, **12** (2023), 695. https://doi.org/10.3390/axioms12070695

21. H. You, Y. Shen, H. Xing, S. Yang, Optimal control and parameters design for the fractional-order vehicle suspension system, *J. Low Freq. Noise Vibration Active Control*, **37** (2018), 456–467. https://doi.org/10.1177/0263092317717166

22. H. Zhu, J. Yang, Y. Zhang, X. Feng, A novel air spring dynamic model with pneumatic thermodynamics, effective friction and viscoelastic damping, *J. Sound Vibration*, **408** (2017), 87–104. https://doi.org/10.1016/j.jsv.2017.07.015

23. J. Niu, J. Hou, Y. Shen, S. Yang, Dynamic analysis and vibration control of nonlinear boring bar with fractional-order model of magnetorheological fluid, *Internat. J. Non-Linear Mech.*, **121** (2020), 103459. https://doi.org/10.1016/j.ijnonlinmec.2020.103459

24. L. Fredette, R. Singh, Effect of fractionally damped compliance elements on amplitude sensitive dynamic stiffness predictions of a hydraulic bushing, *Mech. Syst. Signal Process.*, **112** (2018), 129–146. https://doi.org/10.1016/j.ymssp.2018.04.031

25. G. Wang, L. Ma, A Dynamic behavior analysis of a rolling Mill's main drive system with fractional derivative and stochastic disturbance, *Symmetry*, **15** (2023), 1509. https://doi.org/10.3390/sym15081509

26. L. Jiang, T. Wang, Q. Huang, W. Shi, Study on chaotic characteristics of horizontal nonlinear roller system with fractional order, *Arch. Appl. Mech.*, **93** (2023), 2435–2447. https://doi.org/10.1007/s00419-023-02389-1

27. L. Jiang, T. Wang, Q. Huang, Analysis of dynamic characteristics of forced and free vibrations of mill roll system based on fractional order theory, *J. Beijing Inst. Tech.*, **32** (2023), 640–652. https://doi.org/10.15918/j.jbit1004-0579.2023.051

28. L. Jiang, T. Wang, Q. Huang, Resonance analysis of horizontal nonlinear vibrations of roll systems for cold rolling mills under double-frequency excitations, *Mathematics*, **11** (2023), 1626. https://doi.org/10.3390/math11071626

29. Z. Wang, H. Hu, Stability and bifurcation of delayed dynamic systems: From theory to application, (In Chinese), *Adv. Mech.*, **43** (2013), 3–20. https://doi.org/10.6052/1000-0992-12-018

30. Y. Yan, J. Li, W. Wang, Time-delay feedback control of an axially moving nanoscale beam with time-dependent velocity, *Chaos Solitons Fract.*, **166** (2023), 112949. https://doi.org/10.1016/j.chaos.2022.112949

31. P. Zhu, M. Xiao, X. Huang, F. Zhang, Z. Wang, J. Cao, Spatiotemporal dynamics optimization of a delayed reaction-diffusion mussel-algae model based on PD control strategy, *Chaos Solitons Fract.*, **173** (2023), 113751. https://doi.org/10.1016/j.chaos.2023.113751

32. Y. Shen, H. Li, S. Yang, M. Peng, Y. Han, Primary and subharmonic simultaneous resonance of fractional-order Duffing oscillator, *Nonlinear Dyn.*, **102** (2020), 1485–1497. https://doi.org/10.1007/s11071-020-06048-w

33. R. Caponetto, G. Dongola, L. Fortuna, I. Petras, *Fractional order systems: Modeling and control applications*, World Scientific, 2010. https://doi.org/10.1142/7709

34. I. Petras, *Fractional-order nonlinear systems: Modeling, analysis and simulation*, Heidelberg: Springer Berlin, 2011. http://dx.doi.org/10.1007/978-3-642-18101-6

AIMS Press